



Effect of 1-ethyl-3-methylimidazolium acetate on the oxidation of caffeic acid benzyl ester: An electrochemical and theoretical study

Maurizio A. Pantoja-Hernández | Josué A. Alemán-Vilis | Analilia Sánchez |
Magali Salas-Reyes | Judith López-Bonilla | Myrna H. Matus |
Zaira Domínguez

Unidad de Servicios de Apoyo en Resolución Analítica, Universidad Veracruzana, Xalapa, Mexico

Correspondence

Myrna H. Matus and Zaira Domínguez, Unidad de Servicios de Apoyo en Resolución Analítica, Universidad Veracruzana, Xalapa, Mexico. Email: myhernandez@uv.mx; zdominguez@uv.mx

Funding information

Conacyt-México, Grant/Award Numbers: 134275 and CB-2016-284220

Abstract

The effect of the ionic liquid (IL), 1-ethyl-3-methylimidazolium acetate ([emim][AcO]) on the oxidation of (*E*)-phenylmethyl-3-(3,4-dihydroxyphenyl)-2-propenoate (commonly known as caffeic acid benzyl ester [CABE]) was analyzed through experimental and theoretical methods, such as cyclic voltammetry (CV) and density functional theory (DFT) calculations. The obtained results demonstrated that the AcO[−] anion promotes the oxidation of the caffeic ester; this is because of the basic character of AcO[−], which plays an important role to reduce the amount of energy required for the removal of one electron from the IL-CABE complex. This suggests that a strong hydrogen bond is formed between this anion and the phenolic H—O. Even the presence of water in the mixture of CABE-IL does not have a significant effect on the electrooxidation of the complex. Hence, it is possible to infer that CABE is more attached to [emim][AcO] than to the water molecules in the solvation sphere under the experimental conditions evaluated here. Other intermolecular interactions between CABE and IL also contribute to stabilize the resulting complex, e.g., van der Waals and cation- π interactions, which were evidenced through the theoretical noncovalent interactions (NCI) methodology. The relevant role of basic anions in the extraction of phenolic compounds, using ILs, has been documented in the literature; it should be considered that the strength of the hydrogen bond formed between the phenolic H—O and the IL should not contribute to the oxidation of target compounds.

KEYWORDS

cyclic voltammetry, DFT calculations, extraction processes, ionic liquids, phenolic compounds

1 | INTRODUCTION

Ionic liquids (ILs) are salts with outstanding properties, such as melting temperatures below 100°C, negligible vapor pressure, and high thermal and electrochemical stability.^[1,2] A wide variety of organic and inorganic

compounds as well as polymers are soluble in ILs, hence they are currently recognized as a new class of “green solvents.” In addition, a huge number of organic cations and either organic or inorganic anions are potential candidates for preparing ILs, which allows the possibility to tune their viscosity, toxicity, biodegradation ability, or

hydrophobicity, among other physicochemical properties. Because of their unique characteristics, ILs are applied in synthesis,^[2,3] catalysis and extraction processes.^[4,5] The use of ILs in the extraction of value-added compounds from natural sources has attracted the attention of several research groups.^[6–8] For example, since ILs can dissolve cellulose, they allow an easier access to a wide range of bioactive compounds present in plants such as terpenes, alkaloids, fats, and phenolic compounds.^[6–8]

1-alkyl-3-methylimidazolium is, by far, the most investigated cation used in the extraction of phenolics with ILs; however, the efficiencies of the processes are highly dependent of the anion chosen to form the ionic pair. Guo et al.^[9] examined the solubility of flavonoids in a set of 1888 ILs based on COSMO-RS calculations and found that hydrogen bonding is the dominant interaction between solute and solvent, followed by van de Waals interactions. The general trend showed that ILs with basic character anions, such as those containing acetate, decanoate, and chlorine, were better solvents for flavonoids than those containing BF_4^- , PF_6^- , or Tf_2N^- , regardless of the structure of the cation.

In order to go into detail about the underlying mechanism of ILs—solute interactions at a molecular level, DFT has been used as a valuable tool. For example, Dong et al.^[10] performed a theoretical-experimental study on the interaction between 1-butyl-3-methylimidazolium hexafluorophosphate ($[\text{bmim}][\text{PF}_6]$) and three isoflavone aglycones: genistein, daidzein, and glycitein. The results obtained through DFT calculations showed that in the aglycone-IL complexes, there are hydrogen bonds between the phenolic compounds (except glycitein) and the ion pair; in addition, the authors found a relationship between the experimental distribution coefficients of the isoflavones, in $[\text{bmim}][\text{PF}_6]$, and the strength of the binding energies of PF_6^- -aglycone, which is consistent with a predominant effect of the anion in the stabilization of the aglycone-IL complexes, through an $\text{F}\cdots\text{H}-\text{O}$ hydrogen bond, and with the selectiveness of ILs toward the three solutes. Similar conclusions were reported by Yang et al.^[11] with respect to intermolecular interactions between a series of 1-alkyl-3-methylimidazolium-based ILs and three tocopherols; thus, an anion $\cdots\text{H}-\text{O}$ hydrogen bond (where the anion is Cl^- , Br^- , BF_4^- , AcO^- , Gly^- or Ala^-), as well as weaker interactions of the $\pi-\pi$, $\sigma-\pi$, and van der Waals types were also found between ILs and the phenolic compounds, through NBO analysis.

It is known that 1-ethyl-3-methylimidazolium acetate, $[\text{emim}][\text{AcO}]$, has low toxicity, low corrosiveness, favorable biodegradability, and it can strongly coordinate hydrogen bond donor groups.^[12] Therefore, possible applications of $[\text{emim}][\text{AcO}]$ have been investigated in the last years, particularly with respect to the extraction

of phenolic compounds. Since $[\text{emim}][\text{AcO}]$ is one of the most efficient ILs for obtaining cellulose, hemicellulose, and lignin from biomass,^[13,14] very recently, it was used to recover phenolic compounds dissolved in this salt after being used in a wheat straw pretreatment. Vanillin, vanillic acid, and *p*-coumaric acid, among other phenolic compounds, were identified after a subsequent CO_2 extraction from a $[\text{emim}][\text{AcO}]$ solution.^[15] In addition, a series of aqueous two-phase systems (ATPS) were tested to extract hydroxycinnamic acid derivatives; the one prepared with $[\text{emim}][\text{AcO}]$ and potassium phosphate was the most efficient for extraction of 3,5-*O*- and 4,5-*O*-dicaffeoylquinic acids from stressed carrot tissue, and it was better than ethanol-ammonium sulfate and butanol ammonium sulfate for recovering chlorogenic acid.^[16] On the other hand, through a computational analysis, Zeindlhofer et al.^[17,18] investigated the solvation mechanism for the main constituents of coffee (gallic acid as a representative compound of chlorogenic acid, quercetin, and caffeine) in $[\text{emim}][\text{AcO}]$; in that work, the authors proposed that imidazolium cations are close to the solute surface and, at the same time, they remove water molecules, thus diminishing the interaction between the anion and the coffee constituents due to the hydrophilic character of AcO^- .

The solvation and extraction of phenolic compounds with ILs are still under study. These processes require the use of experimental and theoretical methods to get a better understanding of the phenomena, in order to be more efficient than those using organic solvents. High selectivity and null degradation of the target compounds are crucial parameters to consider in the development of alternative extraction methods using ILs. Hence, extraction of phenolic compounds requires a careful selection of the ion pairs to achieve a strong enough intermolecular interaction without altering the compound structure.

In this work, we apply electrochemical experiments and DFT calculations to describe how $[\text{emim}][\text{AcO}]$ promotes the oxidation of the (*E*)-phenylmethyl-3-(3,4-dihydroxyphenyl)-2-propenoate, also known as caffeic acid benzyl ester (CABE, in Figure 1) in acetonitrile (ACN) or gas phase, as well as the role that intermolecular interactions, between the IL and the ester, play in this process. CABE was chosen as the model compound since it is known that caffeic acid and its natural ester derivatives are found in numerous plants and vegetables,^[19–22] and all of them have strong antioxidant capacity and interesting biological properties.^[23–25] It must be noticed that the labeling used in the figures and tables of this work does not follow the IUPAC rules, however, the proposed labeling is more useful for the corresponding discussion.

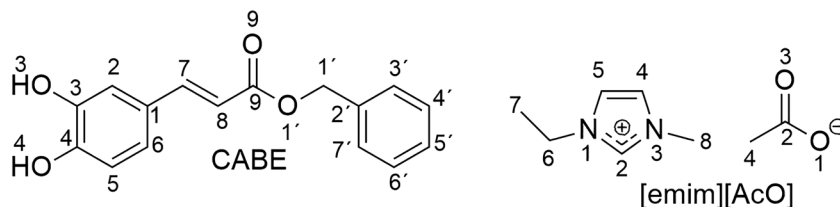


FIGURE 1 Structures of CAFE and [emim][AcO] and atom labelling used in the work

2 | METHODS

2.1 | Instrumentation

^1H and ^{13}C NMR spectra were obtained on an Agilent Technologies 400/54 Premium Shielded (400 MHz) spectrometer, using deuterated ACN (CD_3CN) as solvent. Chemical shifts were recorded in δ (ppm) values from CD_3CN . Signal patterns are indicated as: s, singlet; d, doublet; dd, double doublet; m, multiplet; and br, broad signal. Coupling constants (J) are given in Hertz.

Cyclic voltammetry experiments were performed in a radiometer PGZ-301 (Radiometer Copenhagen) with positive feedback resistance compensation at 25°C , under a high purity nitrogen atmosphere. A Pyrex glass three-electrode cell and a working electrode with a 3-mm diameter glassy carbon disk (Sigradur G from HTW, Germany) were used. Before each run, the polishing of the electrode was made with $1\ \mu\text{m}$ alumina powder, followed by a rinse in an ultrasound bath with distilled water and ethanol. The counter electrode and the reference were a platinum mesh and Ag/AgCl , respectively. A salt bridge containing the same supporting electrolyte concentration, as the working solution, was used to connect the reference electrode to the cell. ACN was bubbled with nitrogen before preparing all the solutions.

2.2 | Chemicals

1-Ethyl-3-methylimidazolium acetate more than or equal to 95%, caffeic acid more than or equal to 98%, benzyl bromide of 98%, tetrabutylammonium hydroxide of 1.0 M, and tetrabutylammonium hexafluorophosphate ($n\text{-Bu}_4\text{NPF}_6$) of 99%, were purchased from Sigma-Aldrich.

ACN (H_2O content less than 0.1%) spectra grade (Merck Uvasol) was used as solvent during the electrochemical experiments. The IL was dried at a reduced pressure using a high vacuum pump at 80°C during 8 hours before use.

Caffeic acid benzyl ester (CABE) was prepared as follows: in a three-necked 100 mL flask fitted with a dropping funnel, stir bar, and rubber septa, 1.0 g (5.5 mmol) of caffeic acid and 40 mL of ACN under nitrogen atmosphere were placed. Thus, 5.5 mL (5.5 mmol) of tetrabutylammonium hydroxide 1.0M were dissolved in

5 mL of ACN and slowly added through the dropping funnel, followed by a solution of 0.68 mL (5.5 mmol) of benzyl bromide in 10 mL of ACN. Stirring was maintained during three more hours at room temperature. After that, the solution was concentrated under vacuum. Purification of the crude product was accomplished by flash chromatography on silica gel using a mixture of 80:20 hexane/EtOAc as eluent. The identity of CABE was determined by NMR spectroscopic data: ^1H NMR (400 MHz) (CD_3CN) δ (ppm): 5.20 (2H, s), 6.35 (1H, d, $^3J_{\text{HH}} = 16$ Hz), 6.84 (1H, d, $^3J_{\text{HH}} = 8$ Hz), 7.02 (1H, dd, $^4J_{\text{HH}} = 2$ Hz and $^3J_{\text{HH}} = 8$ Hz), 7.11 (1H, d, $^4J_{\text{HH}} = 2$ Hz), 7.32–7.44 (5H, m), 7.59 (1H, d, $^3J_{\text{HH}} = 16$ Hz), 8.33 (2H, s, OH). ^{13}C NMR (100 MHz) (CD_3CN) δ (ppm): 66.7, 115.4, 116.0, 116.4, 118.3, 123.0, 128.0, 129.0, 129.5, 137.8, 145.8, 145.9, 148.2, 167.7.

2.3 | Density functional theory calculations

Initial geometry preoptimizations of the IL, CABE, and the IL–CABE complex were carried out in gas phase employing the B3LYP exchange-correlation functional of the density functional theory (DFT) and the DGDZVP2 basis set.^[26–31] For the optimization of the IL, different positions of the anion with respect to the cation were proved; thus, the initial positions were selected by employing the electrostatic potential surfaces of both ions as a reference (electrostatic potential surfaces are shown in Figures S1–S3). In contrast, CABE was optimized using its crystal structure obtained via X-ray diffraction as starting point.^[32]

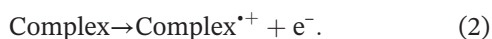
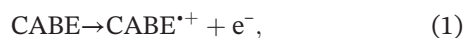
The CABE-IL complex was then optimized employing the lower energy structures (those with $\Delta E_{\text{rel}} < 5$ kcal mol^{-1} , where ΔE_{rel} is the relative energy of the structure) of the IL and CABE. Different initial positions of the IL with respect to CABE were proved, and they were selected by using their electrostatic potential surfaces as a reference. Vibrational frequency calculations were carried out to obtain the zero point energy (ZPE) correction and to ensure that the optimized structures are minima on the potential energy surface. B3LYP calculations for the isolated IL and CABE were performed employing the Gaussian09 software,^[33] whereas calculations for the

complex was carried out using the NWChem 6.6 code^[34] because of the size of the system.

The lowest energy structures of the IL-CABE complex, obtained with B3LYP, were reoptimized at the PBE-D3/6-31++G** level of theory,^[35–40] in order to improve the geometrical and energetic description of the system. The third version of the Grimme dispersion correction was applied to the PBE functional with the aim to obtain a better description of the weak van der Waals interactions.^[41] All the optimizations were followed by frequency calculations. The interaction enthalpies, entropies, and Gibbs energies at 298 K of the complexes were also calculated; in this case, the structures of the isolated IL and CABE were re-optimized at the PBE-D3/6-31++G** level. The basis set superposition error (BSSE) of the interaction energies were corrected applying the counterpoise method.^[42] All the PBE-D3 calculations were performed using the NWChem 6.6 code.

The analysis of the noncovalent interactions was carried out in the optimized complex, as well as in the isolated IL and CABE; in this case, atoms in molecules (AIM) and noncovalent interactions (NCI) methodologies were used.^[43,44] These analyses were performed by the GPU-based code, GPUAM,^[45] with input wave functions obtained from Gaussian09. The search for hydrogen bond interactions was obtained by the getting_HB program,^[46] which uses the information obtained from the AIM analysis (i.e., bond critical points).

The vertical and adiabatic ionization potentials (IP_v and IP_a , respectively) were calculated for the IL-CABE complex and the isolated CABE. The electron removal reactions were as follows.



The IP can be obtained by applying the equation:

$$IP = E_{rc} - E_{neutr}, \quad (3)$$

where E_{rc} is the electronic energy of the radical cation that results from the removal of one electron and E_{neutr} is the electronic energy of the neutral system. For the IP_v , only a single-point calculation was performed to obtain E_{rc} . In contrast, the IP_a considers the geometry optimization of the system when the electron is removed; therefore, the radical cation must be optimized. In addition, frequency calculations were performed in the cases where an optimization was needed. All IP values were calculated in gas phase, at the PBE-D3/6-31++G** level of theory, using the NWChem 6.6 code.

3 | RESULTS AND DISCUSSION

3.1 | Electrochemical study of the [emim][AcO]/CABE interaction

Cyclic voltammetry is an important tool for the antioxidants research since the oxidation potential values obtained through this technique can be used to analyze the electron donating capacity of the studied compounds. It has been shown that there is a relationship between less positive oxidation potentials (i.e., greater capacity to transfer electrons) and higher antioxidant activities.^[47–49]

Figure 2 shows the voltammograms of CABE and a series of [emim][AcO]/CABE mixtures in ACN, where the ratio (R) between both species was varied from 0.49 to 3.70 (IL concentration was varied from 0.98 mM to 7.4 mM, whereas CABE remains at 2 mM in the solution); the black continuous line corresponds to the electrochemical behavior of the neat ester. As it can be observed, a typical chemically irreversible oxidation peak (I) and the corresponding broad reduction wave (II) were registered at 1.08 V and 0.77 V vs Ag/AgCl, respectively.

Similarities between the voltammogram of CABE and those reported before, for caffeic acid and for some of its ester and amides derivatives in aprotic media,^[50–53] allow us to infer that the oxidation of CABE follows an electrochemical-chemical-electrochemical (ECE) mechanism, which involves the loss of an electron from the catechol moiety, followed by a fast deprotonation reaction and the subsequent loss of a second electron.

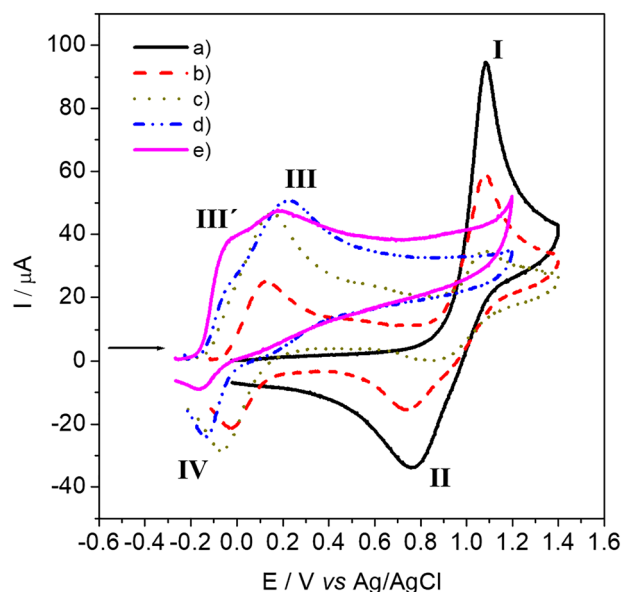
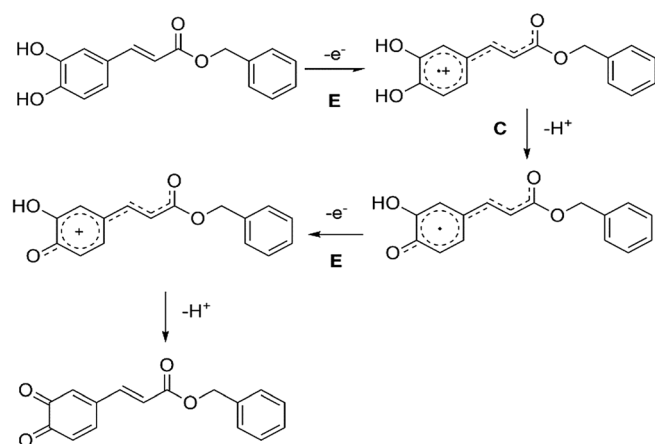


FIGURE 2 Cyclic voltammetry of CABE at 2 mM in ACN + 0.1 M *n*-Bu₄NPF₆ on glassy carbon electrode (3 mm Φ) at 0.1 V s⁻¹ and different concentrations of [emim][AcO]: (A) 0 mM, (B) 0.98 mM, (C) 1.96 mM, (D) 3.98 mM, and (E) 7.4 mM

In the case of caffeoyl derivatives, a further deprotonation has been proposed from experimental evidence, as the last step; this is shown in Scheme 1.^[52]

The voltammogram of a 2 mM solution of neat [emim][AcO] in ACN is shown in Figure 3. In the range between 0 and 2.0 V vs Ag/AgCl, an irreversible oxidation peak **I'** was observed at 1.37 V vs Ag/AgCl, as well as a broad pre-wave **II'** just before peak **I'**. This electrochemical behavior is typical of carboxylate ions (Kolbe reaction) and it has been described in the literature.^[54,55] The oxidation mechanism for this type of anions implies an electronic transfer followed by a decarboxylation (EC). Since the oxidation peak of [emim][AcO] in ACN is 285 mV, which is beyond the oxidation potential of CAFE, an



SCHEME 1 Mechanism electrochemical-chemical-electrochemical (ECE) for the electrochemical oxidation of CAFE

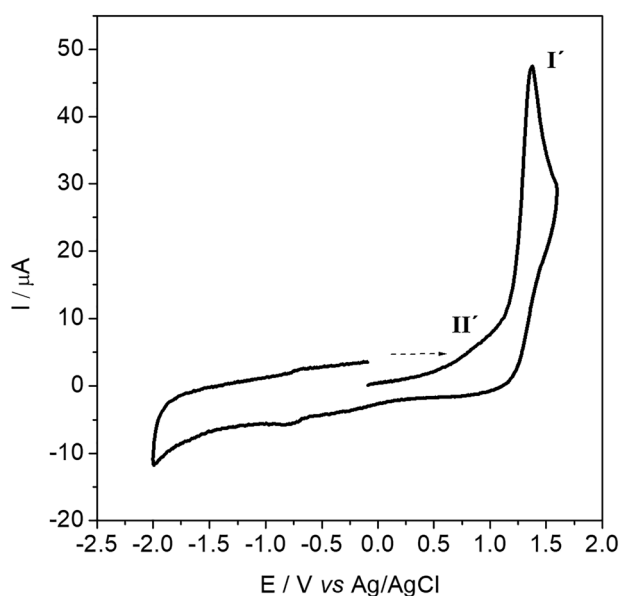


FIGURE 3 Cyclic voltammetry of [emim][AcO] at 2 mM in ACN + 0.1 M *n*-Bu₄NPF₆ on glassy carbon electrode (3 mm Φ) at 0.1 V s⁻¹

overlap of the anodic peaks during the analysis of the mixtures is discarded.

Addition of [emim][AcO] to the CAFE solution produced changes in the electrochemical response, which were dependent on the [emim][AcO]/CAFE ratio (Figure 2). Clearly, the peak intensities of **I** and **II** drop when R is 0.49; in addition, two new peaks, **III** and **IV** (at 0.13 and -0.02 V vs Ag/AgCl, respectively), appear at less anodic potentials. The voltammogram of the solution, with equimolar amounts of both species (Figure 2C), shows that the current intensity of wave **I** is decreased by a third of the initial value, whereas **III** and **IV** became the most important peaks.

A higher concentration of IL (R = 1.90) produced the complete disappearance of the electrochemical response of CAFE (Figure 2D), a decrease and shift of the reduction wave **IV**, and the appearance of a new pre-wave **III'** (-0.04 V vs Ag/AgCl), which becomes more intense when R is 3.70 (Figure 2e). All these changes suggest a strong interaction between CAFE and [emim][AcO], even when the amount of IL is substoichiometric with respect to the ester.

Although the acetate ion presents a basic character, it is not strong enough to remove protons from the ester, considering the pK_a values of acetic acid (23.51) and phenol (29.14) in ACN,^[56,57] which would be closer to that of CAFE. Even in an aqueous media, the proton transfer between both species is not possible, since pK_a values are 4.75 and 8.24 to 8.35 for acetic acid and several caffeic acid esters, respectively.^[58–60]

The electrochemical results of this study provide evidence on the interaction of CAFE with [emim][AcO] by strong hydrogen bonds between the OH groups of the catechol moiety and the acetate ion, thus yielding CAFE-IL complexes whose stoichiometry is defined by the [emim][AcO] concentration. In all these complexes, the anodic peak has a lower value with respect to that of CAFE, which means that they are more susceptible to oxidation. The acetate anion can participate also as an acceptor of the proton during the ECE mechanism described in Scheme 1. In addition, waves **III** and **IV** would be related to complexes where the two OH groups of the ester interact with AcO⁻. That is consistent with the dependence observed between the current intensity of **III** and **IV** as a function of the acetate ion concentration. On the other hand, the pre-wave **III'**, observed at R = 3.70, can be related to the oxidation potential of complexes where each molecule of CAFE interacts with more than two [emim][AcO] ionic pairs.

A similar behavior was observed by Astudillo et al.^[61] in the analysis of the concentration effect of tetrabutylammonium acetate on the electrochemical oxidation of *p*-hydroxyphenol. Interestingly, the authors

were able to perform an X-ray analysis of crystals obtained from a stoichiometric mixture of *p*-hydroxyphenol and the ammonium salt. They found that each acetate ion interacts with two phenol molecules in the solid state by strong O—H...O hydrogen bonds, which reinforces the conclusions achieved from electrochemical data.

Since the extraction processes using ILs are commonly performed in an aqueous solution, the effect of water on the electrochemical oxidation of CAGE and CAGE-IL complexes was also investigated. Figure 4 shows a series of voltammograms corresponding to the titrations of a neat CAGE solution with different concentrations of water (from 0 to 532.9 mM). As it can be observed, a slight decrease in the current intensities of peaks I and II was noticeable when the H₂O/CAGE ratio increased; this is consistent with a reduction of the diffusion coefficient for the electroactive species because of the formation of a complex involving CAGE and molecules of water, probably achieved by intermolecular hydrogen bonds. In addition, both peaks move to less anodic potentials when the water concentration reaches 57 mM; in the case of peak I, it shifts by a difference of approximately 90 mV when the water concentration is 533 mM (H₂O/CAGE ratio = 266).

Figure 5 shows the voltammograms of the H₂O/CAGE mixture (ratio = 266) in the presence of different concentrations of [emim][AcO] (from 0.5 mM to 2.8 mM). The electrochemical behavior is practically the same as the one observed in Figure 2. Nevertheless, when water is

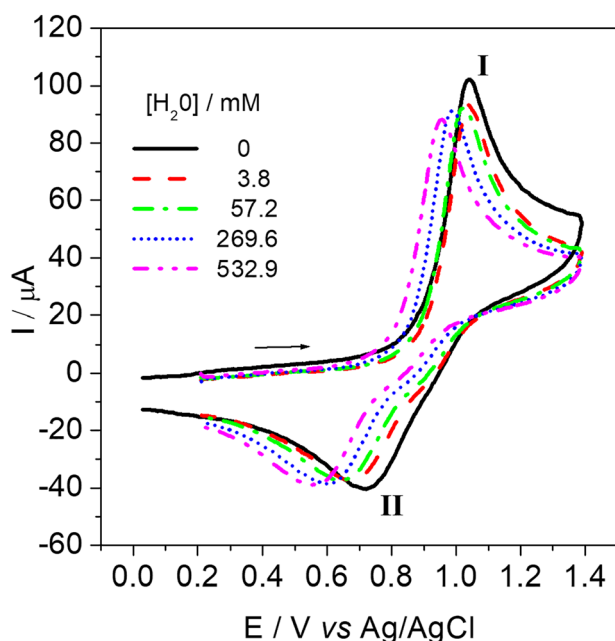


FIGURE 4 Cyclic voltammetry of CAGE at 2 mM in ACN + 0.1 M *n*-Bu₄NPF₆ on glassy carbon electrode (3 mm Φ) at 0.1 V s⁻¹ at different concentrations of H₂O

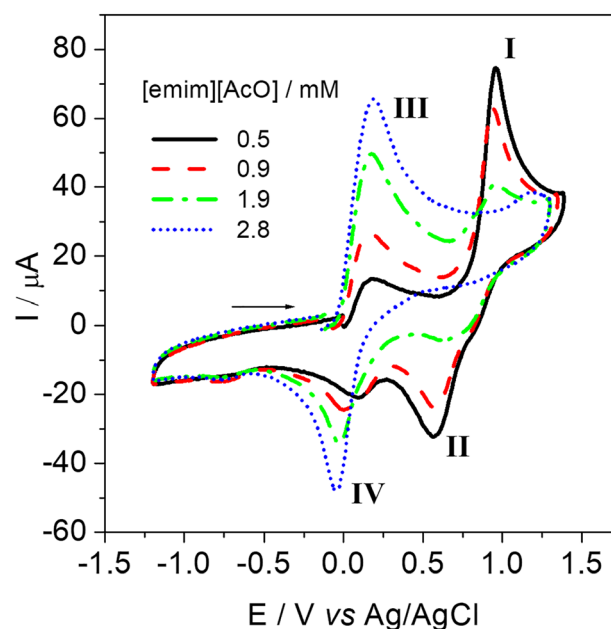


FIGURE 5 Cyclic voltammetry of CAGE at 2 mM in ACN + 0.1 M *n*-Bu₄NPF₆ + 0.532.9 M H₂O on glassy carbon electrode (3 mm Φ) at 0.1 V s⁻¹ at different concentrations of [emim][AcO]

present, peak IV increases as the amount of IL becomes higher, and it does not disappear as described in the voltammograms of CAGE-IL mixtures. These results suggest that water stabilizes the oxidation products of the CAGE-IL complexes, which allow them to remain close to the electrode surface, for a longer time, before the potential is inverted to register its electrochemical reduction.

From the experiments shown in Figures 4 and 5, it can be concluded that the electrochemical oxidation of CAGE and CAGE-IL complexes are not significantly affected by the presence of water since the hydrogen bonds formed by H₂O with both type of species are weak. Even more, water is not able to replace the AcO⁻ anion around the phenolic hydroxyl groups of CAGE. Thus, under these experimental conditions, it seems that CAGE is closer to [emim][AcO] than to the water molecules in the solvation sphere.

3.2 | Theoretical results

In order to gain more insight into the noncovalent interactions present in the CAGE-IL complex, AIM^[43] and NCI^[44] analyses were performed at the PBE-D3/6-31++G** level of calculation for the optimized structures. Similarly, such analyses were applied to the optimized structures of the isolated IL and CAGE with the aim to compare between the interactions in an isolated form and the interactions in the complexes.

The AIM methodology allows to determine if two nuclei are bonded (either by a covalent bond or a noncovalent interaction) by taking into account topological features of the electron density ($\rho(r)$). The presence of a bond critical point (BCP) and a bond path in the region between two nuclei of a system, with a minimum energy equilibrium geometry, indicates that the two atoms are bonded. Thus, a BCP is a point where the electron density gradient ($\nabla\rho(r)$) becomes zero, whereas a bond path is a line that connects two nuclei where $\rho(r)$ is a maximum with respect to any neighboring line.^[62] To determine the nature of a bond, e.g., if it is covalent or noncovalent, the properties of $\rho(r)$ and its derivatives at the corresponding BCP are considered.^[43,62]

On the other hand, the NCI index uses $\rho(r)$ and its reduced gradient (s) to identify noncovalent interactions in the real space.^[44] Noncovalent interactions are characterized as regions with low values of both $\rho(r)$ and s , thus they can be identified in the real space by mapping them as low- s isosurfaces subject to the constraint of having low values of $\rho(r)$ (reduced density gradient s versus sign(λ_2) ρ profiles for the studied structures are shown in Figures S4-S7). To distinguish between attractive and repulsive interactions, the value of $\rho(r)$ is multiplied by the sign of the second eigenvalue (λ_2) of the density Hessian (this multiplication is denoted as sign(λ_2) ρ , where sign(λ_2) $\rho < 0$ indicates attractive interactions and sign(λ_2) $\rho > 0$ indicates repulsive interactions.^[44,63] The NCI-reduced gradient isosurfaces are colored according to the value of sign(λ_2) ρ . For this work, a blue-green-red color scale was used for the NCI isosurfaces (see Scheme 2), where the blue-colored surfaces indicate strong attractive interactions, the green-colored isosurfaces describe weak attractive interactions, and the red-colored surfaces indicate strong repulsive interactions.

Figure 6 shows the results of AIM and NCI analyses for the isolated IL. The BCPs are indicated as pink-colored points, whereas the bond paths are shown as pink-colored lines. Hydrogen bonds can be identified by the presence of both a BCP and a bond path between the H atom and the acceptor atom.

The values of $\rho(r)$ and its Laplacian ($\nabla^2\rho(r)$) at the BCP are also important criteria for the identification of

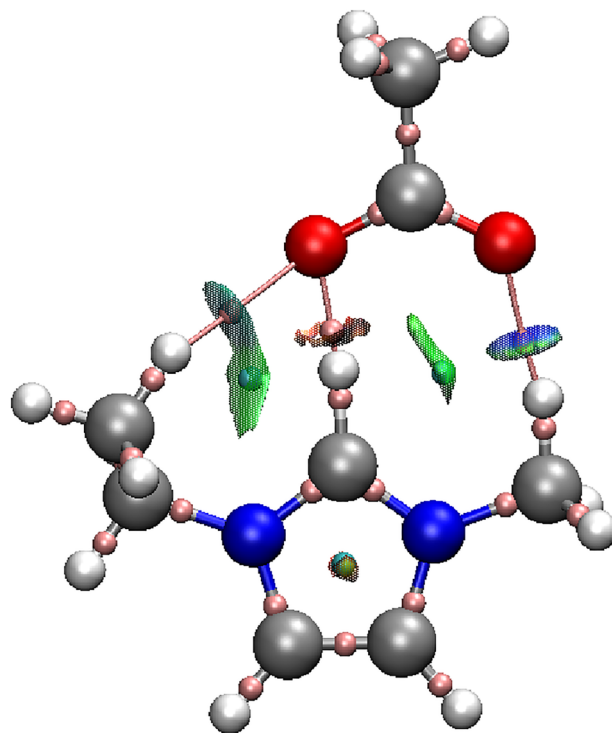


FIGURE 6 Atoms in molecules (AIM) and noncovalent interactions (NCI) analyses for the isolated [enim][AcO]. The bond critical points are shown as pink-colored points and the bond paths as pink-colored lines. The cyan-colored points are ring critical points. The blue-colored surfaces indicate strong attraction interactions, whereas the green-colored surfaces indicate weak van der Waals interactions. The red-colored surfaces indicate repulsive interactions

hydrogen bonds, where $\rho(r)$ should be in the range of 0.002 to 0.034 a.u., whereas $\nabla^2\rho(r)$ should be positive and in the range of 0.024 to 0.139 a.u., as proposed by Koch and Popelier.^[64]

The geometrical parameters of the hydrogen bond interactions found in the isolated IL are shown in Table 1.

The values of $\rho(r)$, $\nabla^2\rho(r)$ at their BCPs, as well as their respective estimated energies, are shown in Table 2. The hydrogen bond energies (E_{HB}) were calculated by considering the empirical relationship between E_{HB} and the electronic potential energy density (or virial field) at the corresponding BCP ($V(r_{\text{BCP}})$), as proposed by Espinosa et al.^[65] (see Equation 1).



Strong
attractive
interactions

Weak
attractive
interactions:
van der Waals,
dispersion

Strong
repulsive
interactions

SCHEME 2 Color scale employed for noncovalent interactions (NCI)-reduced gradient isosurfaces

TABLE 1 Geometrical parameters of the hydrogen bond interactions found in the isolated [emim][AcO]

Atoms Involved		Geometrical Parameters		
Cation	Anion	H...A distance, Å	D...A distance, Å	D-H...A angle, °
C2-H2	O1	1.546	2.712	170.89
C8-H8	O3	1.974	3.071	168.64
C7-H7	O1	2.373	3.371	149.69

Abbreviation: A, acceptor atom; D, donor atom.

TABLE 2 Values of $\rho(r)$ and $\nabla^2\rho(r)$ at the BCPs, and energies of the hydrogen bond interactions found in the isolated [emim][AcO]

Atoms Involved		$\rho(r)$ au]	$\nabla^2\rho(r)$, au	Energy, kcal mol ⁻¹
Cation	Anion			
C2-H2	O1	0.0733	0.1449	-19.17
C8-H8	O3	0.0266	0.0701	-5.93
C7-H7	O1	0.0110	0.0367	-2.40

$$E_{\text{HB}} = V(r_{\text{BCP}})/2, \quad (4)$$

where $V(r_{\text{BCP}})$ is obtained from the AIM analysis.

For [emim][AcO] (Figure 6), three hydrogen bond interactions were found, each one of which involves one of the O atoms of the acetate anion and either H2, H7, or H8 of the [emim] cation (see labeling for the atoms in Figure 1). Nevertheless, the strongest interaction is the hydrogen bond between the anion and the H2 atom of the imidazolium ring (see Table 2).

For the isolated CABE (Figure 7), an intramolecular hydrogen bond interaction between H4 and O3 was found (see labeling for the atoms of CABE in Figure 1). This interaction presents an H-acceptor distance of 2.15 Å and a donor-hydrogen-acceptor angle of 113.64°. The estimated energy for this interaction is -4.80 kcal mol⁻¹.

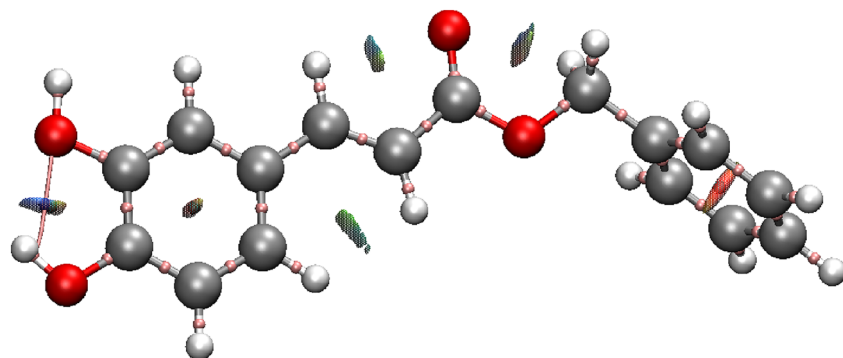
**FIGURE 7** Atoms in molecules (AIM) and noncovalent interactions (NCI) analyses for the isolated CABE. The bond critical points are shown as pink-colored points and the bond paths as pink-colored lines. The cyan-colored points are ring critical points. The blue-colored surfaces indicate strong attraction interactions, whereas the green-colored surfaces indicate weak van der Waals interactions. The red-colored surfaces indicate repulsive interactions

Figure 8 shows the results of AIM and NCI analyses for the [emim][AcO]-CABE complex. In general, 11 BCPs that correspond to noncovalent interactions, with their corresponding bond paths, were found in this system. For all these BCPs, the values of $\nabla^2\rho(r)$ are positive, which is typical of closed-shell interactions, such as hydrogen bonds, van der Waals, and ionic interactions.^[62]

Considering the previously mentioned criteria for the identification of hydrogen bonds, seven interactions of this kind were found in the complex. Geometrical parameters of the identified hydrogen bond interactions, as well as the values of $\nabla^2\rho(r)$ and $\rho(r)$ at their BCPs, as well as their estimated energies, are shown in Table 3.

As it can be observed from Table 3, the strongest interaction in the complex is the hydrogen bond between one of the O atoms of the anion (O3) and the H atom of one of the hydroxyl groups of CABE (O3-H3). The estimated energy for this interaction is -32.69 kcal mol⁻¹, which is significantly stronger than the rest of the hydrogen bonds in the system. On the other hand, the value of $\rho(r)$ at its corresponding BCP is 0.0962 a.u. which is higher than the upper limit of the range proposed by Koch and Popelier for hydrogen bonds (0.002-0.034 a.u.)^[64] and it is close to the values corresponding to covalent bonds (in the order of 10⁻¹ a.u.).^[62]

The two strongest hydrogen bond interactions between the anion and the cation of the isolated [emim][AcO] are also present in the formation of the [emim][AcO]-CABE complex, C2-H2...O1 and C6-H6...O3; in both cases, their strength decreases by 10.8 kcal mol⁻¹ and 1.84 kcal mol⁻¹, respectively (see Tables 1 and 3). The C2-H2...O1 interaction is the second strongest in the system and it is 24.32 kcal mol⁻¹ weaker than the previously mentioned O3-H3...O3 hydrogen bond between CABE and the anion (see Table 3). In contrast, the intramolecular hydrogen bond that occurs in the isolated CABE is also present in the complex (O4-H4...O3) and it is strengthened by 1.47 kcal mol⁻¹ when the complex is formed.

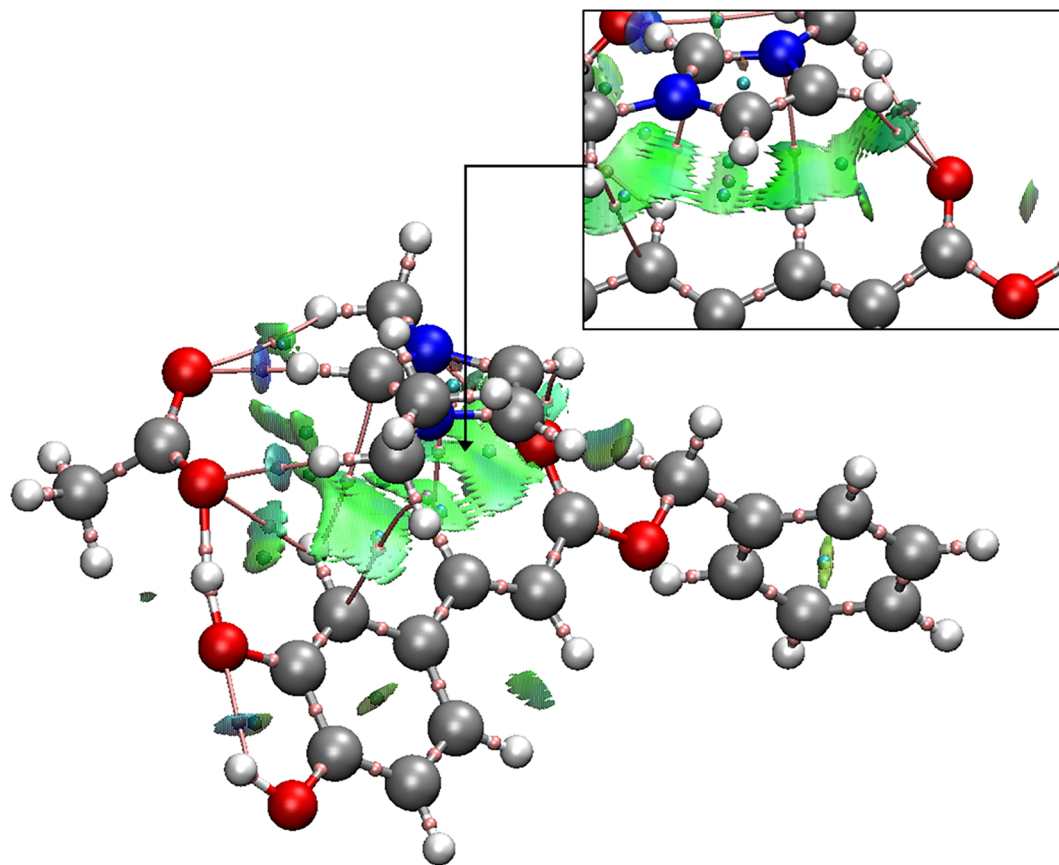


FIGURE 8 Atoms in molecules (AIM) and noncovalent interactions (NCI) analyses for the [emim][AcO]-CABE complex. The bond critical points are shown as pink-colored points and the bond paths as pink-colored lines. The cyan-colored points are ring critical points. The blue-colored surfaces indicate strong attraction interactions, while the green-colored surfaces indicate weak van der Waals interactions. The red-colored surfaces indicate repulsive interactions

TABLE 3 Geometrical parameters, values of $\rho(r)$ and $\nabla^2\rho(r)$ at the BCPs and energies of the hydrogen bond interactions found in the [emim][AcO]-CABE complex

Atoms Involved			Geometrical Parameters			BCP Parameters		
Cation	Anion	CABE	H...A distance, Å	D...A distance, Å	D-H...A angle, °	$\rho(r)$, a.u.	$\nabla^2\rho(r)$, a.u.	Energy, kcal mol ⁻¹
	O3	O3-H3	1.416	2.479	169.83	0.0962	0.1121	-32.69
C2-H2	O1		1.821	2.890	159.02	0.0380	0.0962	-8.37
		O4-H4, O3	2.033	2.645	118.07	0.0238	0.0849	-6.27
C6-H6	O3		2.165	3.193	154.05	0.0182	0.0513	-4.09
C8-H8	O9		2.383	3.312	141.16	0.0108	0.0363	-2.31
	O3	C2-H2	2.529	3.182	117.26	0.0103	0.0346	-2.11
C4-H4	O9		2.531	3.132	113.88	0.0093	0.0337	-1.83

Abbreviations: A, acceptor atom; D, donor atom

On the other hand, Figure 8 shows the presence of a wide green-colored NCI isosurface between the cation and the caffeoyl moiety of CABE. This result suggests an interaction of the aromatic ring and the conjugated double bond with the imidazolium ion. In addition, the analysis indicates that H4 and H8 of the imidazolium ring

interact with the carbonyl group of CABE because of the presence of hydrogen bonds (see zoomed-in region in Figure 8), with energies approximately 2 kcal mol⁻¹ in both cases.

Four intermolecular BCPs that do not meet the criteria for hydrogen bond interactions were found in the

complex, two of which are C—H...C interactions between CAFE and the cation, and the other two are a C—H...N interaction between the same two species and a C—H...O interaction between the cation and the anion of the IL. The BCPs for these interactions possess values of $\rho(r)$ in the order of 10^{-3} a.u. and are associated to the green-colored isosurface between CAFE and the cation; this indicates that in addition to the cation- π type, van der Waals interactions could also be present.^[62,66]

The thermochemical parameters, at 298 K, for the formation of the [emim][AcO]-CAFE complex, applying the PBE-D3/6-31++G** level of theory (including BSSE) in gas phase are: $\Delta H_m = -32.22$ kcal mol⁻¹, $\Delta G_m = -8.93$ kcal mol⁻¹, and $\Delta S_m = -78.10$ cal mol⁻¹ K⁻¹. Theoretical results predict that the formation process at 298 K is spontaneous and it is close to the thermodynamic equilibrium ($\Delta G_m \pm 10$ kcal mol⁻¹). This fact would be convenient for the subsequent separation of the phenolic compound from the IL since only low amounts of energy must be applied to carry out the process. Nevertheless, in the experimental conditions explored in this study, [emim][AcO] promotes the oxidation of the caffeic ester before that can be done.

In contrast, the removal of one electron from the complex (Complex → Complex⁺⁺ + e⁻), at the same level of calculation and T = 298 K, is a very endothermic and nonspontaneous process: $\Delta H_m = 141.82$ kcal mol⁻¹ and $\Delta G_m = 142.32$ kcal mol⁻¹. As a comparison with the neutral [emim][AcO]-CAFE complex, Figure 9 shows the results of AIM and NCI analyses for the [emim][AcO]-CAFE complex once one electron has been removed. In this figure, it can be observed that nine BCPs that correspond to noncovalent interactions, with their corresponding bond paths, were found in this system; in addition, a

reduction of the green isosurface (see NCI results) can be appreciated between the CAFE structure and the [emim]⁺ ion.

The most drastic change between Figures 8 and 9 can be seen in the strongest hydrogen bond found in both structures. In Figure 8, the O3 atom of the anion is forming a very strong hydrogen bond with H3—O3 of the CAFE molecule (O3...H3—O3); in contrast, this interaction is different in Figure 9 since the hydrogen is now attached to the AcO⁻ anion, thus showing a proton transfer from CAFE, where the hydrogen-acceptor distance (see Table 4) O3—H3...O3 is of 1.623 Å with a corresponding interaction energy of -13.69 kcal mol⁻¹, i.e., 9 kcal mol⁻¹ weaker than the neutral structure. It must be noticed that the value of $\rho(r)$, at its corresponding BCP, is 0.0561 a.u. which is higher than the upper limit for hydrogen bonds (0.002-0.034 a.u.),^[64] however, it is closer to a hydrogen bond value than to those corresponding to covalent bonds (approximately 10⁻¹ a.u.).^[62]

In addition, the hydrogen bonds resulting from the cation-anion interaction of the IL, C2—H2...O1, and C6—H6...O3 diminish their strength by 2.58 and 2.15 kcal mol⁻¹, respectively; it must be noticed that the [AcO]⁻ ion is, actually, not an ion since the proton transfer turned it into acetic acid. Finally, the complete stabilization of the [emim][AcO]-CAFE complex, once an electron is removed, can be achieved if it is considered that the other hydrogen bond interactions become slightly stronger by less than 0.4 kcal mol⁻¹ (see Tables 3 and 4).

On the other hand, calculations of the ionization potential (adiabatic and vertical, IP_a and IP_v , respectively) for the removal of an electron were carried out in the isolated CAFE and the IL-CAFE complex, these results are shown in Table 5. As it can be observed, the complex

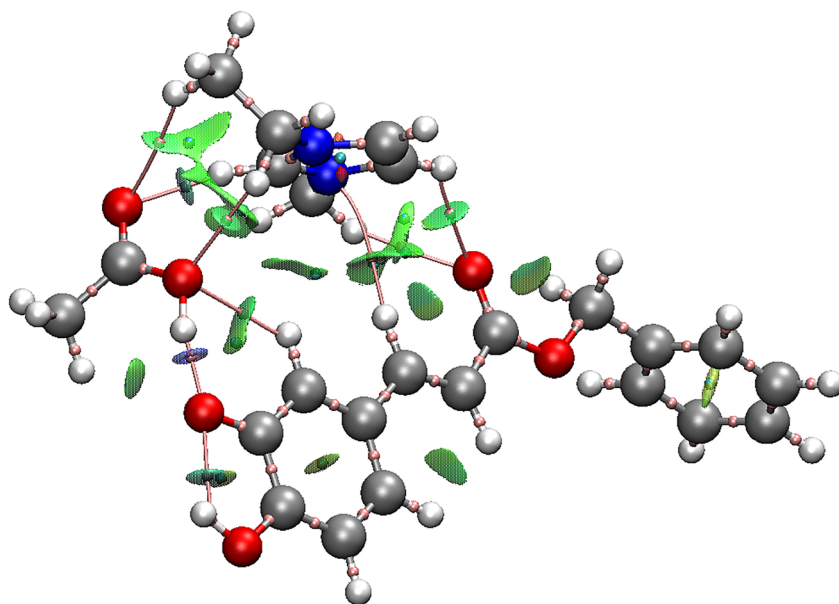


FIGURE 9 Atoms in molecules (AIM) and noncovalent interactions (NCI) analyses for the [emim][AcO]-CAFE complex once an electron was removed. The bond critical points are shown as pink-colored points and the bond paths as pink-colored lines. The cyan-colored points are ring critical points. The blue-colored surfaces indicate strong attraction interactions, while the green-colored surfaces indicate weak van der Waals interaction

TABLE 4 Geometrical parameters, values of $\rho(r)$ and $\nabla^2\rho(r)$ at the BCPs and energies of the hydrogen bond interactions found in the [emim][AcO]-CABE⁺⁺ complex

Atoms Involved			Geometrical Parameters			BCP Parameters		
Cation	Anion	CABE	H...A distance, Å	D...A distance, Å	D-H...A angle, °	$\rho(r)$, a.u.	$\nabla^2\rho(r)$, a.u.	Energy, kcal mol ⁻¹
	O3-H3(tp)	O3	1.623	2.620	164.36	0.0561	0.1386	-13.69
		O4-H4, O3	2.030	2.643	117.57	0.0257	0.0834	-6.56
C2-H2	O1		1.977	3.040	161.60	0.0262	0.0681	-5.79
C8-H8		O9	2.366	3.329	145.24	0.0114	0.0367	-2.45
C4-H4		O9	2.396	3.162	126.23	0.0105	0.0381	-2.22
	O3	C2-H2	2.451	3.197	124.27	0.0105	0.0354	-2.19
C6-H6	O3		2.493	3.354	134.08	0.0094	0.0314	-1.94

Abbreviations: A, acceptor atom; D, donor atom; tp, transferred proton.

TABLE 5 Values of IP_a and IP_v for the removal of an electron from CABE and from the IL-CABE complex and IP_a and IP_v differences between CABE and the complex in kcal mol⁻¹

System	IP_a (IP_v)	ΔIP_a (ΔIP_v) (Complex vs CABE)
CABE	168.07 (170.34)	
[emim][AcO]-CABE	141.09 (155.48)	-26.98 (-14.86)

has lower IP_a and IP_v than the isolated CABE, which indicates that the amount of energy required to remove an electron from the system decreases in comparison with the neat caffeic ester. This result agrees with the electrochemical data discussed above and predicts that, in gas phase, the [emim][AcO] promotes the oxidation of the phenolic compound because of the IL capacity to interact with the electroactive unit of the caffeic ester.

4 | CONCLUSIONS

The caffeic acid benzyl ester (CABE) compound, belonging to one of the groups of phenolic compounds ubiquitous in the plant kingdom, interacts with [emim][AcO], mainly through a strong hydrogen bond located between one of the phenolic hydrogens of the ester and the anion of the IL, nonetheless other noncovalent interactions are also present, such as van der Waals and cation- π . Theoretical data suggest that, whereas the anions remain fixed to the phenolic hydrogen, the imidazolium rings are stacked over the caffeoyl moiety in the IL-CABE complex. Even the carboxylic oxygen participates in the formation of hydrogen bonds since it interacts with H4 and H8 from the imidazolium cation in the [emim][AcO]-CABE complex. Because of these stabilizing interactions, calculations predict that the formation of the complex is slightly exergonic at 298 K and close to the

thermodynamic equilibrium, i.e., ΔG_m is approximately 10 kcal mol⁻¹. From these results, it can be said that [emim][AcO] might be a good candidate to be used in the extraction of caffeic acid derivatives from natural products. Nevertheless, the IL-CABE complex is more susceptible to oxidation than neat CABE, particularly because of the basic character of AcO⁻, at least in ACN, and gas phase. Electrochemical experiments and theoretical calculations coincide in the following: the strongest hydrogen bond O-H...OAc, present in the complex, promotes the removal of one electron from the electroactive catechol moiety at a lower energy in comparison with the neat ester. In addition, the presence of water in the CABE-IL mixture, does not have a significant effect on the electrooxidation of the complexes. Hence, it is possible to infer that CABE is closer to the IL, [emim][AcO], than to the water molecules in the solvation sphere under the experimental conditions evaluated in this work.

Thus, in the search of ILs for efficient extractions of phenolic compounds, it must be taken into consideration that the strength of the O-H...anion interaction must be strong enough without contributing to the oxidation of the target compounds. For this purpose, cyclic voltammetry and computational chemistry are excellent tools of analysis. In the best of our knowledge, this is the first time that the effect of ionic liquids on the oxidation of phenolic compounds is reported.

ACKNOWLEDGEMENTS

M.H.M. and M.S.R. thank Conacyt-México for grant nos. CB-2016-284220 and 134275, respectively. M.A.P.H. thanks Conacyt-México for the Master scholarship, no. 423214. Authors gratefully acknowledge the *Laboratorio Nacional de Cómputo de Alto Desempeño* (LANCAD) at the *Universidad Autónoma Metropolitana-Iztapalapa* for access to *Yollla* (supercomputer).

CONFLICT OF INTEREST

There are no conflict to declare.

ORCID

Maurizio A. Pantoja-Hernández  <https://orcid.org/0000-0002-0663-1001>

Josué A. Alemán-Vilis  <https://orcid.org/0000-0002-7638-5950>

Magali Salas-Reyes  <https://orcid.org/0000-0002-9358-8944>
Judith López-Bonilla  <https://orcid.org/0000-0002-1054-3135>

Myrna H. Matus  <https://orcid.org/0000-0003-2538-7400>

Zaira Domínguez  <https://orcid.org/0000-0002-1224-7217>

REFERENCES

- [1] T. Welton, *Chem. Rev.* **1999**, *99*, 2071.
- [2] H. Weingärtner, *Angew. Chem. Int. Ed.* **2008**, *47*, 654.
- [3] M.-C. Tseng, H.-T. Cheng, M.-J. Shen, Y.-H. Chu, *Org. Lett.* **2011**, *13*, 4434.
- [4] A. Aupoix, B. Pégot, G. Vo-Thanh, *Tetrahedron* **2010**, *66*, 1352.
- [5] Y. Fan, Y. Li, X. Dong, G. Hu, S. Hua, J. Miao, Z. Dongdong, *Ind. Eng. Chem. Res.* **2014**, *53*, 20024.
- [6] H. Passos, M. G. Freire, J. A. P. Coutinho, *Green Chem.* **2014**, *16*, 4786.
- [7] S. P. M. Ventura, F. A. E. Silva, M. V. Quental, D. Mondal, M. G. Freire, J. A. P. Coutinho, *Chem. Rev.* **2017**, *117*, 6984.
- [8] M. G. Bogdanov, in *Alternative Solvents for Natural Products Extraction*, (Eds: F. Chemat, M. A. Vian), Springer-Verlag, Berlin **2014**, Ch. 7 127.
- [9] Z. Guo, B. M. Lue, K. Thomasen, A. S. Meyer, X. Xu, *Green Chem.* **2007**, *9*, 1362.
- [10] K. Dong, Y. Cao, Q. Yang, S. Zhang, H. Xing, Q. Ren, *Ind. Eng. Chem. Res.* **2012**, *51*, 5299.
- [11] Q. Yang, H. Xing, B. Su, Z. Bao, J. Wang, Y. Yang, Q. Ren, *AIChE* **2013**, *59*, 1657.
- [12] H. F. D. Almeida, H. Passos, J. A. Lopes-da Silva, A. M. Fernandez, M. G. Freire, J. A. P. Coutinho, *J. Chem. Eng. Data* **2012**, *57*, 3005.
- [13] A. M. da Costa Lopes, K. G. João, E. Bogel-Lukasik, L. B. Roseiro, R. Bogel-Lukasik, *J. Agric. Food Chem.* **2013**, *61*, 7874.
- [14] A. M. da Costa Lopes, K. G. João, D. F. Rubik, E. Bogel-Lukasik, L. Duarte, J. Andraus, R. Bogel-Lukasik, *Bioresour. Technol.* **2013**, *142*, 198.
- [15] A. M. da Costa Lopes, M. Brenner, P. Falé, L. B. Roseiro, R. Bogel-Lukasik, *ACS Sustain. Chem. Eng.* **2016**, *4*, 3357.
- [16] J. C. Sánchez-Rangel, D. A. Jacobo-Velázquez, L. Cisneros-Zevallos, J. Benavides, *J. Chem. Technol. Biotechnol.* **2016**, *91*, 144.
- [17] V. Zeinlhofer, M. Berger, O. Steinhauser, C. Schröder, *J. Chem. Phys.* **2018**, *148*, 193819.
- [18] V. Zeindlhofer, D. Khlan, K. Bica, C. Schröder, *RSC Adv.* **2017**, *7*, 3495.
- [19] H. F. Harrison, J. K. Peterson, M. E. Snook, J. R. Bohac, D. M. Jackson, *J. Agric. Food Chem.* **2003**, *51*, 2943.
- [20] P. Mattila, J. Kumpulainen, *J. Agric. Food Chem.* **2002**, *50*, 3660.
- [21] N. X. Nhiem, K. C. Kim, A.-D. Kim, J. W. Hyun, K. Kang, P. V. Kiem, C. V. Minh, V. K. Thu, B. H. Tai, J. A. Kim, Y. H. Kim, *J. Asian, Nat. Prod. Res.* **2011**, *13*, 56.
- [22] Y. Lu, X. Li, H. Mu, H. Huang, G.-P. Li, Q. Hu, *J. Braz. Chem. Soc.* **2012**, *23*, 656.
- [23] F. M. da Cunha, D. Duma, J. Assreuy, F. C. Buzzi, R. Niero, M. M. Campos, J. B. Calixto, *Free Radic. Res.* **2004**, *38*, 1241.
- [24] H. G. Choi, P. T. Tran, J.-H. Lee, B. S. Min, J. A. Kim, *Arch. Pharm. Res.* **2018**, *41*, 64.
- [25] X. Guo, I. Shen, Y. Tong, J. Zhang, G. Wu, Q. He, S. Yu, X. Ye, L. Zou, Z. Zhang, X. Y. Lian, *Phytomed.* **2013**, *20*, 904.
- [26] A. D. Becke, *J. Chem. Phys.* **1993**, *98*, 5648.
- [27] P. J. Stephens, F. J. Devlin, C. F. Chabalowski, M. J. Frisch, *J. Phys. Chem.* **1994**, *98*, 11623.
- [28] P. Hohenberg, W. Kohn, *Phys. Rev.* **1964**, *136*, B864.
- [29] W. Kohn, L. J. Sham, *Phys. Rev.* **1965**, *140*, A1133.
- [30] N. Godbout, D. R. Salahub, *Can. J. Chem.* **1992**, *70*, 560.
- [31] J. Andzelm, E. Wimmer, *J. Chem. Phys.* **1992**, *96*, 1280.
- [32] O. Martínez-Mora, Bachelor in Sciences Thesis Universidad Veracruzana (Mexico) **2013**.
- [33] M. J. Frisch, G. W. Trucks, H. B. Schlegel, G. E. Scuseria, M. A. Robb, J. R. Cheeseman, G. Scalmani, V. Barone, B. Mennucci, G. A. Petersson, H. Nakatsuji, M. Caricato, X. Li, H. P. Hratchian, A. F. Izmaylov, J. Bloino, G. Zheng, J. L. Sonnenberg, M. Hada, M. Ehara, K. Toyota, R. Fukuda, J. Hasegawa, M. Ishida, T. Nakajima, Y. Honda, O. Kitao, H. Nakai, T. Vreven, J. A. Montgomery Jr., J. E. Peralta, F. Ogliaro, M. Bearpark, J. J. Heyd, E. Brothers, K. N. Kudin, V. N. Staroverov, T. Keith, R. Kobayashi, J. Normand, K. Raghavachari, A. Rendell, J. C. Burant, S. S. Iyengar, J. Tomasi, M. Cossi, N. Rega, J. M. Millam, M. Klene, J. E. Knox, J. B. Cross, V. Bakken, C. Adamo, J. Jaramillo, R. Gomperts, R. E. Stratmann, O. Yazyev, A. J. Austin, R. Cammi, C. Pomelli, J. W. Ochterski, R. L. Martin, K. Morokuma, V. G. Zakrzewski, G. A. Voth, P. Salvador, J. J. Dannenberg, S. Dapprich, A. D. Daniels, O. Farkas, J. B. Foresman, J. V. Ortiz, J. Cioslowski, D. J. Fox, *Gaussian 09*, Revision A.01, Gaussian, Inc., Wallingford CT **2009**.
- [34] M. Valiev, E. J. Bylaska, N. Govind, K. Kowalski, T. P. Straatsma, H. J. J. Van Dam, D. Wang, J. Nieplocha, E. Apra, T. L. Windus, W. A. De Jong, *Comput. Phys. Commun.* **2010**, *181*, 1477.
- [35] J. P. Perdew, K. Burke, M. Ernzerhof, *Phys. Rev. Lett.* **1996**, *77*, 3865.
- [36] J. P. Perdew, K. Burke, M. Ernzerhof, *Phys. Rev. Lett.* **1997**, *78*, 1396.
- [37] W. J. Hehre, R. Ditchfield, J. A. Pople, *J. Chem. Phys.* **1972**, *56*, 2257.
- [38] P. C. Hariharan, J. A. Pople, *Theoret. Chim. Acta (Berl.)* **1973**, *28*, 213.
- [39] M. M. Francl, W. J. Pietro, W. J. Hehre, J. S. Binkley, M. S. Gordon, D. J. DeFrees, J. A. Pople, *J. Chem. Phys.* **1982**, *77*, 3654.
- [40] M. J. Frisch, J. A. Pople, *J. Chem. Phys.* **1984**, *80*, 3265.

- [41] S. Grimme, J. Antony, S. Ehrlich, H. Krieg, *J. Chem. Phys.* **2010**, *132*, 154104.
- [42] S. F. Boys, F. Bernardi, *Mol. Phys.* **1970**, *19*, 553.
- [43] R. F. W. Bader, *Chem. Rev.* **1991**, *91*, 893.
- [44] E. R. Johnson, S. Keinan, P. Mori-Sánchez, J. Contreras-García, A. J. Cohen, W. Yang, *J. Am. Chem. Soc.* **2010**, *132*, 6498.
- [45] R. Hernández-Esparza, S. M. Mejía-Chica, A. D. Zapata-Escobar, A. Guevara-García, A. Martínez-Melchor, J. M. Hernández-Pérez, R. Vargas, J. Garza, *J. Comput. Chem.* **2014**, *35*, 2272.
- [46] J. Garza, H. B. Getting, *Program for the Search of Hydrogen Bond Interactions From AIM Data*, Universidad Autónoma Metropolitana, Mexico City (Mexico) **2018**.
- [47] M. Born, P.-A. Carrupt, R. Zini, F. Brée, J.-P. Tillement, K. Hostettmann, B. Testa, *Hel. Chim. Acta* **1996**, *79*, 1147.
- [48] H. Hotta, S. Nagano, M. Ueda, Y. Tsujino, J. Koyama, T. Osakai, *Biochim. Biophys. Acta* **2002**, *1572*, 123.
- [49] M. C. Foti, C. Daquino, C. Geraci, *J. Org. Chem.* **2004**, *69*, 2309.
- [50] P. Hapiot, A. Neudeck, J. Pinson, H. Fulcrand, P. Neta, C. Rolando, *J. Electroanal. Chem.* **1996**, *405*, 169.
- [51] R. Petrucci, P. Astolfi, L. Greci, O. Firuzi, L. Saso, G. Marrosu, *Electrochim. Acta* **2007**, *52*, 2461.
- [52] M. Salas-Reyes, J. Hernández, Z. Domínguez, F. J. González, P. D. Astudillo, R. E. Navarro, E. Martínez-Benavidez, C. Velázquez-Contreras, S. Cruz-Sánchez, *J. Braz. Chem. Soc.* **2011**, *22*, 693.
- [53] A. Sánchez, O. Martínez-Mora, E. Martínez-Benavides, J. Hernández, Z. Domínguez, M. Salas-Reyes, *Org. Biomol. Chem.* **2014**, *12*, 5981.
- [54] C. P. Andrieux, F. González, J.-M. Saveant, *J. Electroanal. Chem.* **2001**, *498*, 171.
- [55] M. Galicia, F. J. González, *J. Electrochem. Soc.* **2002**, *149*, D46.
- [56] A. Kütt, I. Leito, I. Kaljurand, L. Sooväli, V. M. Vlasov, L. M. Yagupolskii, I. A. Koppe, *J. Org. Chem.* **2006**, *71*, 2829.
- [57] A. Kütt, V. Movchun, T. Rodima, T. Dansauer, E. B. Rusanov, I. Leito, I. Kaljurand, J. Koppel, V. Pihl, I. Koppel, G. Ovsjannikov, L. Toom, M. Mishima, M. Medebielle, E. Lork, G.-V. Rösenthaller, I. A. Koppel, A. A. Kolomeitsev, *J. Org. Chem.* **2008**, *71*, 2607.
- [58] F. G. Bordwell, *Acc. Chem. Res.* **1988**, *21*, 456.
- [59] M. Penhoat, *Tetrahedron Lett.* **2013**, *54*, 2571.
- [60] F. A. M. Silva, F. Borges, C. Guimarães, J. L. F. C. Lima, C. Matos, S. Reis, *J. Agric. Food Chem.* **2000**, *48*, 2122.
- [61] P. D. Astudillo, J. Tiburcio, F. J. González, *J. Electroanal. Chem.* **2007**, *604*, 57.
- [62] P. L. A. Popelier, *Atoms in Molecules: An Introduction*, Prentice-Hall, Harlow **2000** 144.
- [63] J. Contreras-García, W. Yang, *J. Phys. Chem. A* **2011**, *115*, 12983.
- [64] U. Koch, P. L. A. Popelier, *J. Phys. Chem.* **1995**, *99*, 9747.
- [65] E. Espinosa, E. Molins, C. Lecomte, *Chem. Phys. Lett.* **1998**, *285*, 170.
- [66] R. G. A. Bone, R. F. W. Bader, *J. Phys. Chem.* **1996**, *100*, 10892.

SUPPORTING INFORMATION

Additional supporting information may be found online in the Supporting Information section at the end of the article.

How to cite this article: Pantoja-Hernández MA, Alemán-Vilis JA, Sánchez A, et al. Effect of 1-ethyl-3-methylimidazolium acetate on the oxidation of caffeic acid benzyl ester: An electrochemical and theoretical study. *J Phys Org Chem.* 2019;e4044. <https://doi.org/10.1002/poc.4044>